Electronic Supplementary Information

Experiment Section

Materials

Most of the reagents are from Maclin Biochemical Technology Co., Ltd. (Shanghai, China), including ammonium fluoride (NH_4F), ferric nitrate nonahydrate ($Fe(NO_3)_3·9H_2O$), ethylenediaminetetraacetic acid disodium ($C_{10}H_{14}N_2Na_2O_8$), sodium hydroxide (NaOH), potassium phosphate monobasic (KH_2PO_4), N, N-diethyl-p-phenylenediamine (DPD), urea, disodium phosphate anhydrous (Na_2HPO_4), and nickel nitrate hexahydrate ($Ni(NO_3)_2·6H_2O$). From Beijing Chemical Reagent Co., Ltd., we bought ethanol and hydrochloric acid (HCl). Potassium hydroxide (KOH), Nafion (5 wt%), ruthenium oxide (RuO_2), sodium chloride (NaCl), vanadium trichloride (VCl_3), sodium carbonate anhydrous (Na_2CO_3), and Pt/C (20 wt% Pt) were all acquired from Shanghai Aladdin Co., Ltd. The supplier of the Ni foam (NF) utilized in the research was Xingtai's Qingyuan Metal Materials Co., Ltd. A Millipore system was used to purify the ultrapure (UP) water used in the experiments. No further purification was necessary because the chemical was used as supplied.

Synthesis of NiFe LDH/NF and V-NiFe LDH/NF

Initially, a 2.0 × 3.0 cm^2 nickel foam substrate was ultrasonically cleaned for 15 minutes in three different media: 3 M HCl, ultrapure water, and ethanol. After cleaning, the NF was placed in a Teflon-lined autoclave and submerged in a 40 mL aqueous precursor solution containing $Fe(NO_3)_3·9H_2O$ (1 mmol), $CO(NH_2)_2$ (10 mmol), $Ni(NO_3)_2·6H_2O$ (2 mmol), and NH_4F (4 mmol). For 6 h, the hydrothermal synthesis was carried out at 120 °C. After naturally cooling to room temperature, the NiFe LDH/NF sample was removed from the autoclave, cleaned with ultrapure water, and dried at 60 °C. V-NiFe LDH/NF was made using the same procedure, but the precursor solution was supplemented with 0.1 mmol VCl_3.

Preparation of RuO_2/NF and Pt/C/NF

5 mg of RuO_2 (or 20 wt.% Pt/C) was ultrasonically dispersed for 30 minutes to create a homogenous catalyst ink (final concentration: 5 mg mL^{-1}) in a mixed solution including 485 μL of deionized water, 30 μL of Nafion and 485 μL of ethanol. A clean nickel foam (NF; 0.5 x 0.5 cm^2) substrate was then drop-cast with 300 μL of the ink, resulting in a loading of 6 mg

cm^{-2}.

Preparation of alkaline seawater

First, 6.8 g of Na_2CO_3 was added to 1 L of natural seawater under stirring. The mixture was then left to stand for half a day and subjected to vacuum filtration. Subsequently, 1 M KOH was added to 1 L of the filtrate. After standing overnight, the mixture was centrifuged to obtain alkaline seawater with a pH of 14.

Characterization

X-ray diffraction (XRD) data were collected on a Philips D8 powder diffractometer equipped with Cu Kα radiation source. The morphological features and elemental distribution of the as-prepared catalysts were characterized by a scanning electron microscope (SEM, ZEISS Gemini SEM 300) integrated with an energy-dispersive X-ray (EDX) spectroscopy system operating at 5 kV. An ESCALAB 250 Xi spectrometer was employed to conduct X-ray photoelectron spectroscopy (XPS) measurements, which enabled the analysis of surface chemical compositions and valence states of constituent elements. Meanwhile, a Horiba Lab RAM HR Evolution microscope with 532 nm excitation was used to measure Raman spectra, and a UV–visible (UV–vis) spectrophotometer (Shimadzu UV-2700) was used to examine light absorption properties.

Electrochemical test

Electrochemical assays targeting the OER performance were conducted using a Chenhua CHI660E electrochemical workstation, which adopted a standard three-electrode assembly. To be more precise, a carbon rod served as the counter electrode, a Hg/HgO electrode was chosen as the reference electrode, and the newly manufactured catalyst sample with a geometric area of 0.5 × 0.5 cm^2 served as the working electrode. Linear sweep voltammetry (LSV) curves were collected under quasi-steady-state conditions, covering a potential interval from 0 to 1.4 V (vs. Hg/HgO) at a fixed scan rate of 5 mV s^{-1}. In a separate set of experiments, electrochemical impedance spectroscopy (EIS) characterizations were executed in an electrolyte composed of 1 M KOH and seawater, with the AC amplitude configured at 1 mV and the frequency swept over the range of 10^5 to 10^{-2} Hz. All measured potentials, with the exception of the data in Fig. 4e, S7 and S11, were converted to the reversible hydro-gen

electrode (RHE) scale using the formula $E_{RHE} = E_{Hg/HgO} + 0.098 + 0.059 \times pH$ and iR-compensated using the correction Ec = E – iR (Ec is iR-compensated potential, E is the original potential, i is the corresponding current, and R is the solution resistance). Cyclic voltammetry (CV) measurements at scan rates between 20 and 120 mV s^{-1} were used to quantify the double-layer capacitance (Cdl). Electrolytes with a pH of around 14 were used for all measurements.

Turnover frequency (TOF) calculation

The TOF is evaluated based on the concentration of active sites and calculated using: TOF = A*j*/4Fm. Here, A represents the geometric area of the test electrode, *j* denotes current density, 4 signifies the moles of electron consumption for one mole of O_2 evolution, F is the Faradic constant (96,485 C mol^{-1}), and m represents the number of active sites (mol). The value of m can be determined from the linear relationship between the oxidation peak currents and scan rate using the equation: Slope = $n^2F^2m/4RT$, with n assuming an electron transfer number of 1 for a single-electron process involving the oxidation of the metal center in the catalyst.

Determination of active chlorine

The concentration of active chlorine in the electrolyte was determined using a UV-vis spectrophotometer in conjunction with the DPD colorimetric method (J. G. Vos and M. T. M. Koper, *J. Electroanal. Chem.*, 2018, **819**, 260–268). To initiate the analysis, 100 μL of the electrolyte, which had undergone a long-term stability test at 1000 mA cm^{-2}, was sequentially mixed with 50 μL of 1.0 M H_2SO_4, 50 μL of 2.0 M NaOH, and 4.8 mL of deionized water. Subsequently, 250 μL of DPD reagent and 250 μL of PBS (pH 6.5) were added to the solution, resulting in the development of a pink color. The active chlorine concentrations were analyzed through UV-vis absorption spectrometry at 550 nm.

Fabrication of AEM electrolyzer

The AEM was comprised of a cathode and an anode with a geometric area of 1 cm^2. The prepared electrodes of V-NiFe LDH/NF and Pt/C/NF were selected as OER and HER electrodes, respectively. The cell was fed with 1 M KOH + seawater flowing at a fixed

velocity of 50 mL min^{-1}. The full-cell performance was carried out at room temperature, and the data was recorded on the CHI 660E analyzer.

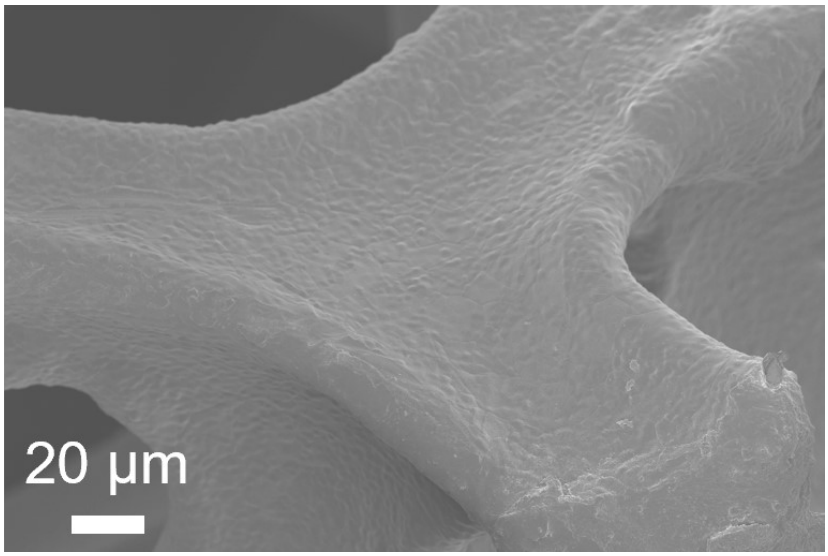

Fig. S1. SEM image of NF.

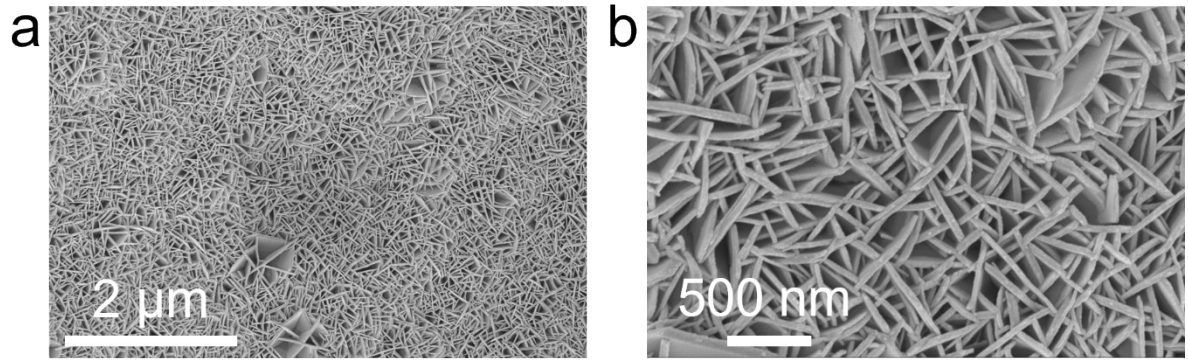

Fig. S2. (a) Low-and (b) high-magnification SEM images of NiFe LDH/NF.

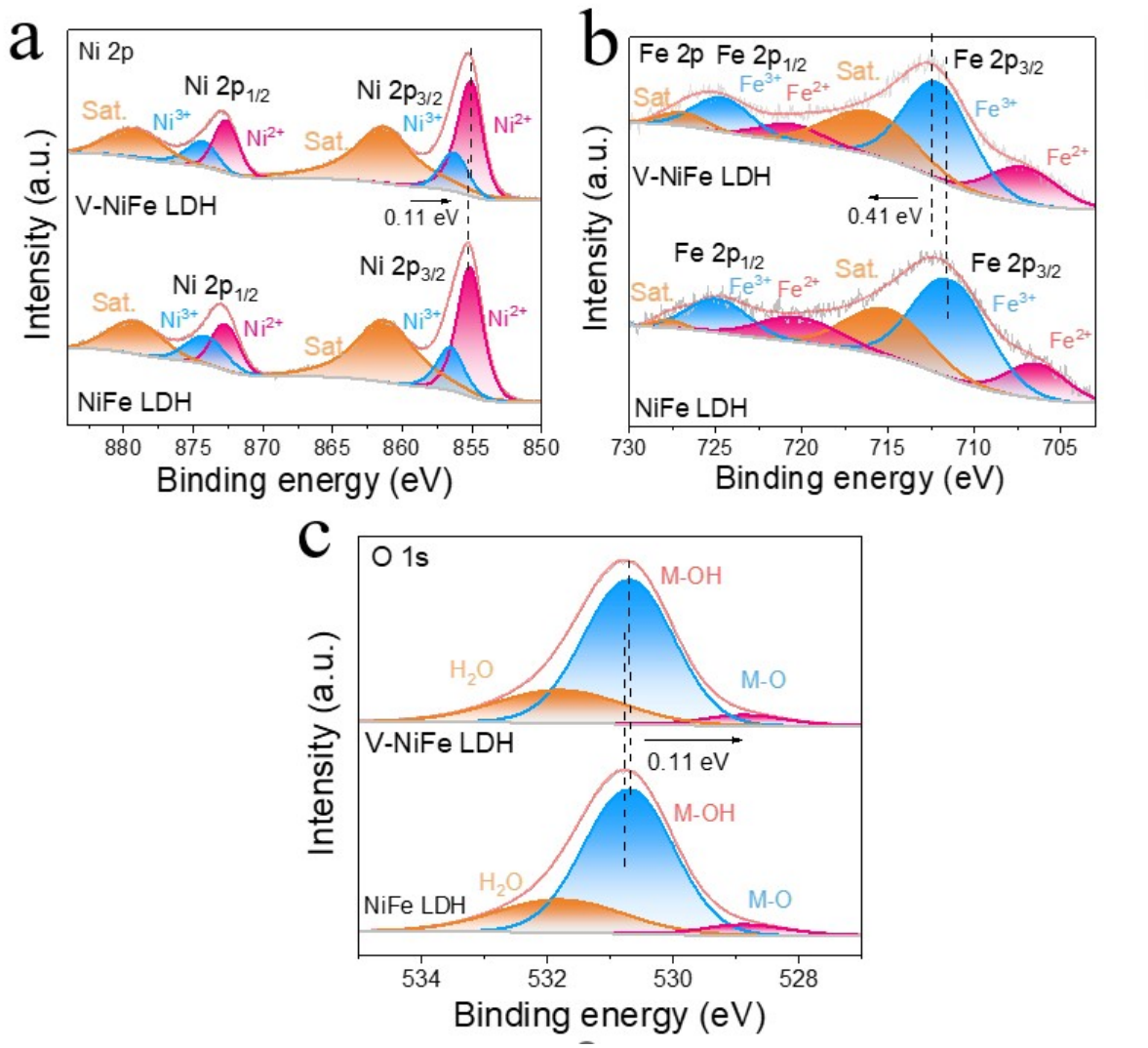

Fig. S3. XPS spectra of V-NiFe LDH and NiFe LDH in the (a) Ni 2p, (b) Fe 2p, and (c) O 1s regions.

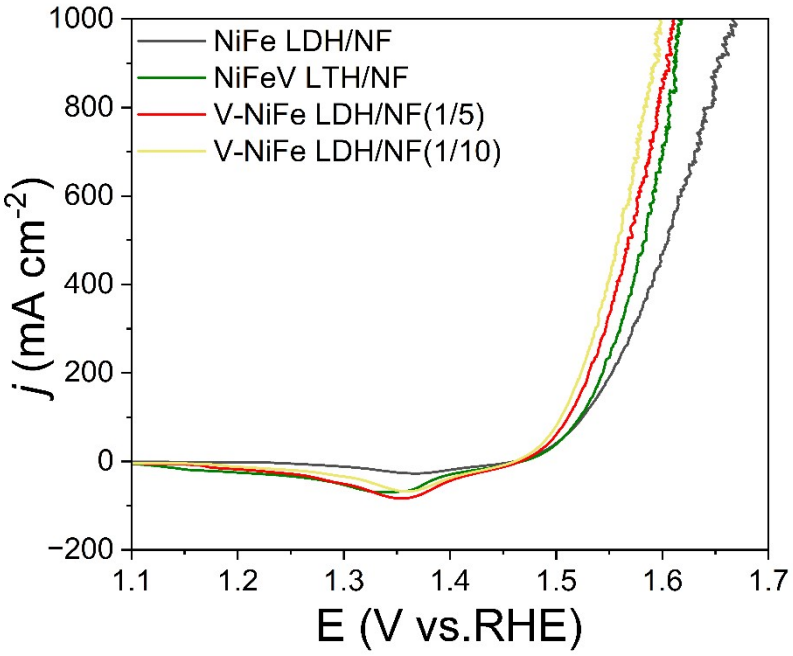

Fig. S4. LSV curves for V-NiFe LDH/NF in 1 M KOH + seawater.

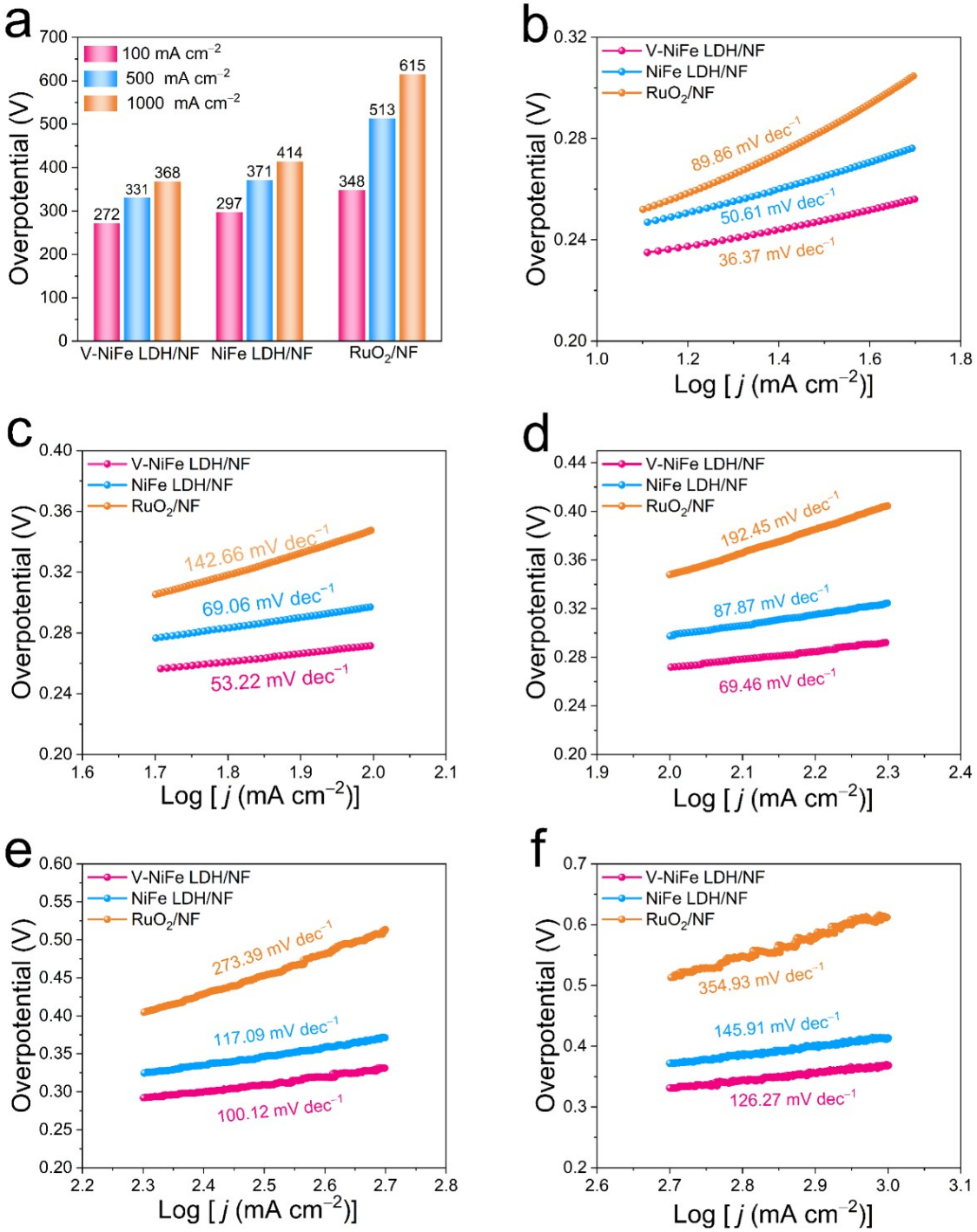

Fig. S5. (a) Overpotential comparison and Tafel plots of V-NiFe LDH/NF, NiFe LDH/NF, RuO_2/NF at different current density ranges (b) 10–50, (c) 50–100, (d) 100–200, (e) 200–500, and (f) 500–1000 mA cm^{-2}

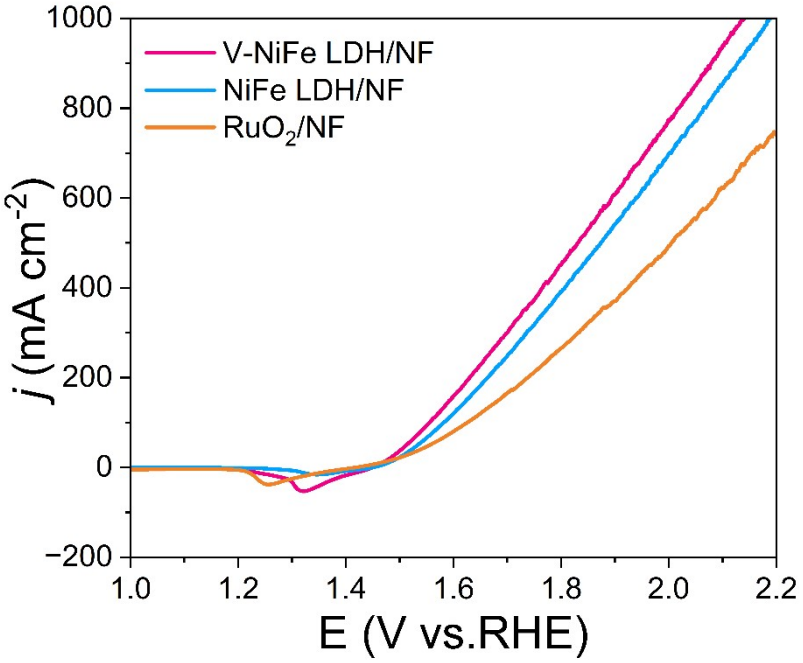

Fig. S6. LSV curves of different electrodes without iR compensation in 1 M KOH + seawater.

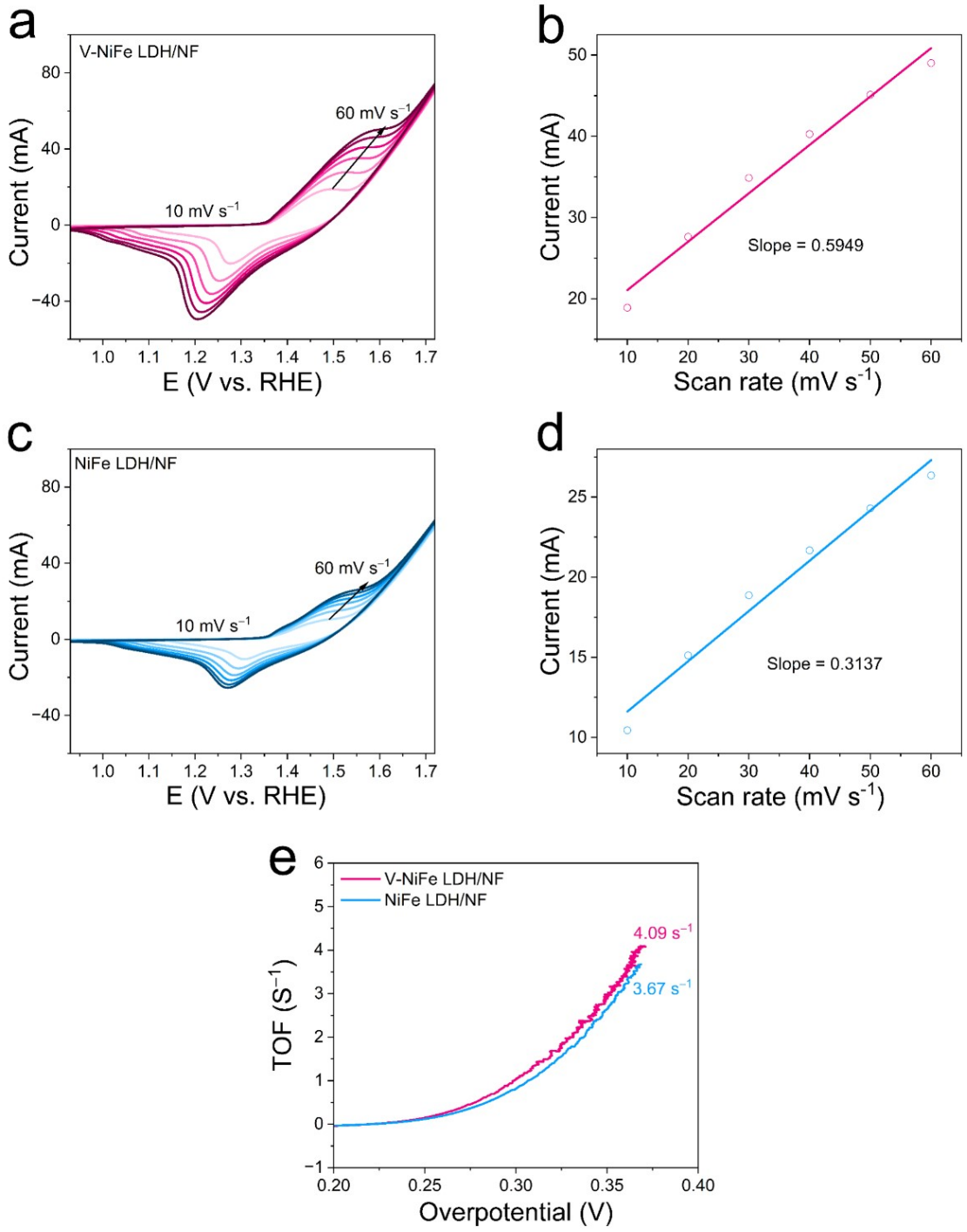

Fig. S7. CV curves for (a) V-NiFe LDH/NF and (c) NiFe LDH/NF at different scan rates increasing from 5 to 60 mV s^{-1} in 1 M KOH + seawater. Oxidation peak current versus scan rate plots for (b) V-NiFe LDH/NF, (d) NiFe LDH/NF (e) TOF plots of V-NiFe LDH/ NF, NiFe LDH/NF.

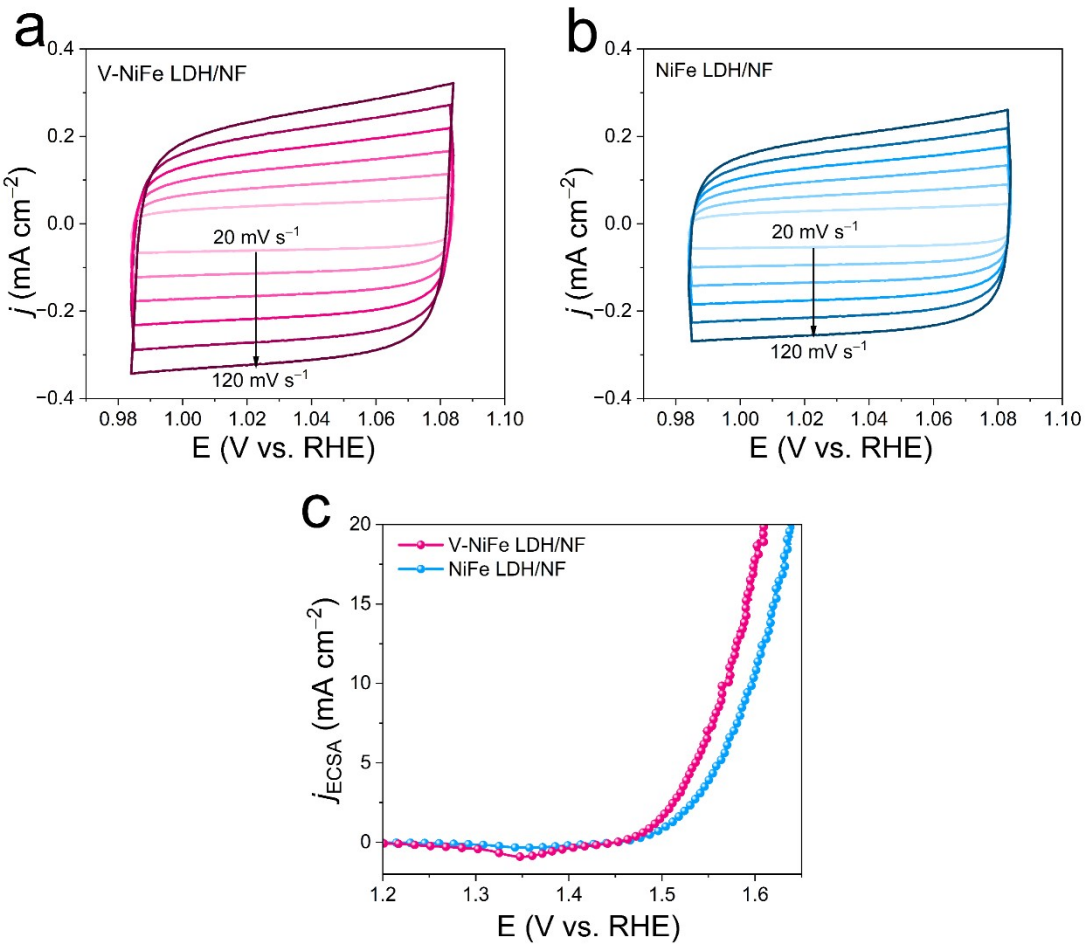

Fig. S8. CV curves of (a) V-NiFe LDH /NF and (b) NiFe LDH/NF in the double layer region at different scan rates of 20, 40, 60, 80, 100, and 120 mV s^{-1} in 1 M KOH + seawater. (c)LSV curves in 1 M KOH + seawater for V-NiFe LDH/NF, NiFe LDH/NF normalized by the electrochemical active surface area.

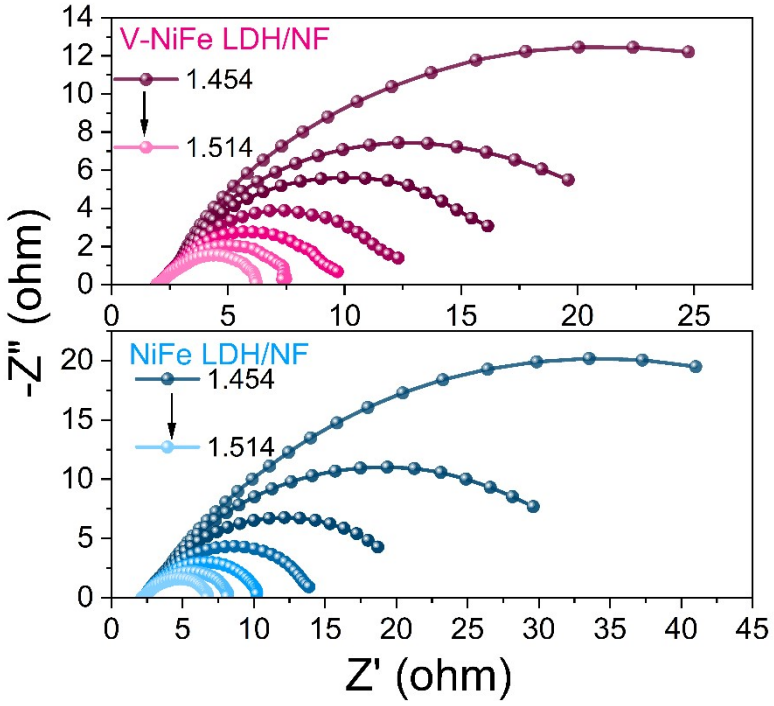

Fig. S9. Nyquist plots at various potentials of V-NiFe LDH/NF and NiFe LDH/NF.

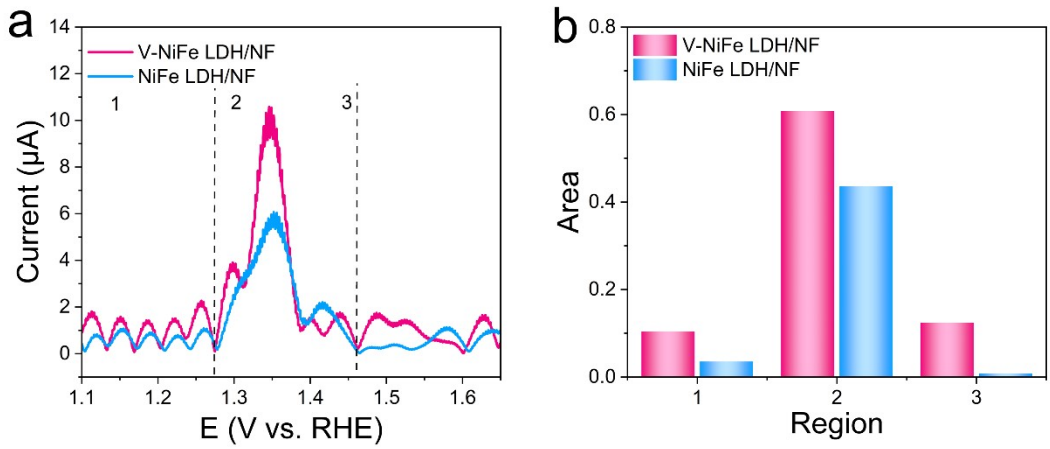

Fig. S10. (a) FTacV curves and (b) corresponding regions area of V-NiFe LDH/NF and NiFe LDH/NF.

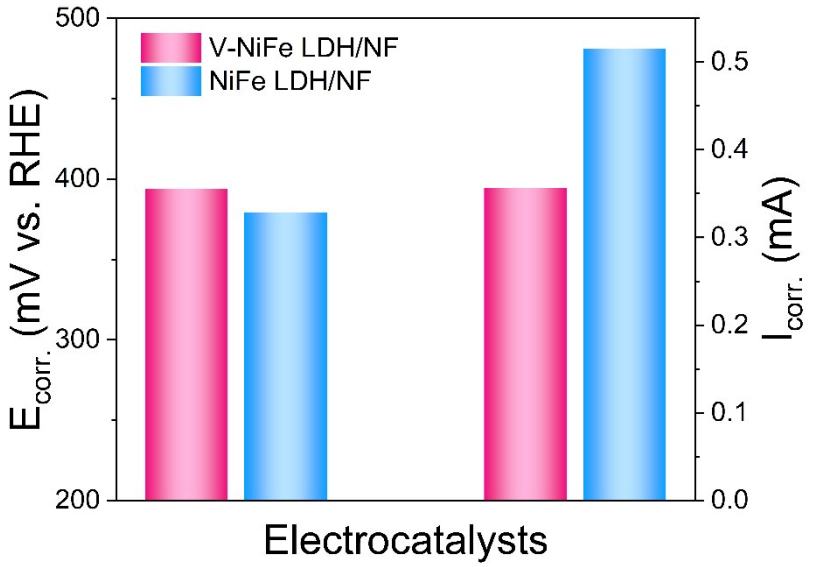

Fig. S11. Comparison of $E_{corr.}$ and $I_{corr.}$ of V-NiFe LDH/NF and NiFe LDH/NF in 1 M KOH + seawater.

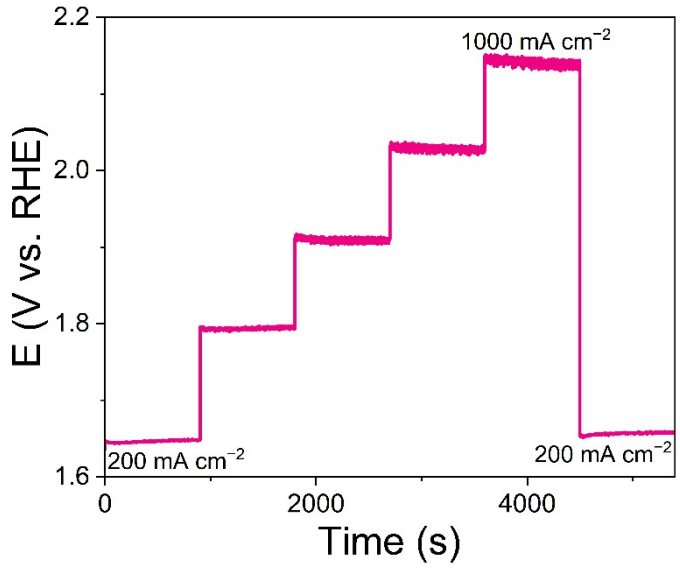

Fig. S12. The multistep chronopotentiometry curve of V-NiFe LDH/NF without iR correction in 1 M KOH + seawater.

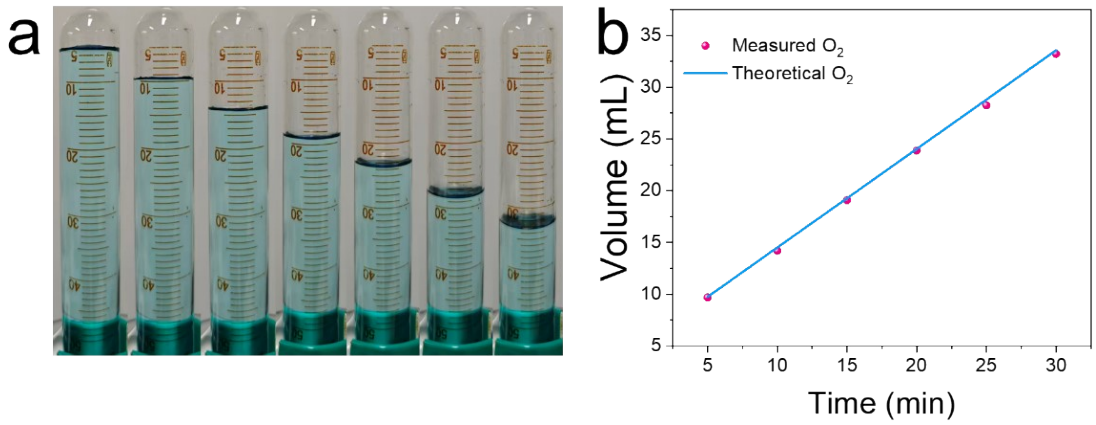

Fig. S13. (a) Collection of oxygen evolved from seawater oxidation at the *j* of 1000 mA cm^{-2} by the water drainage method. (b) The volume of O_2 is calculated theoretically and measured experimentally.

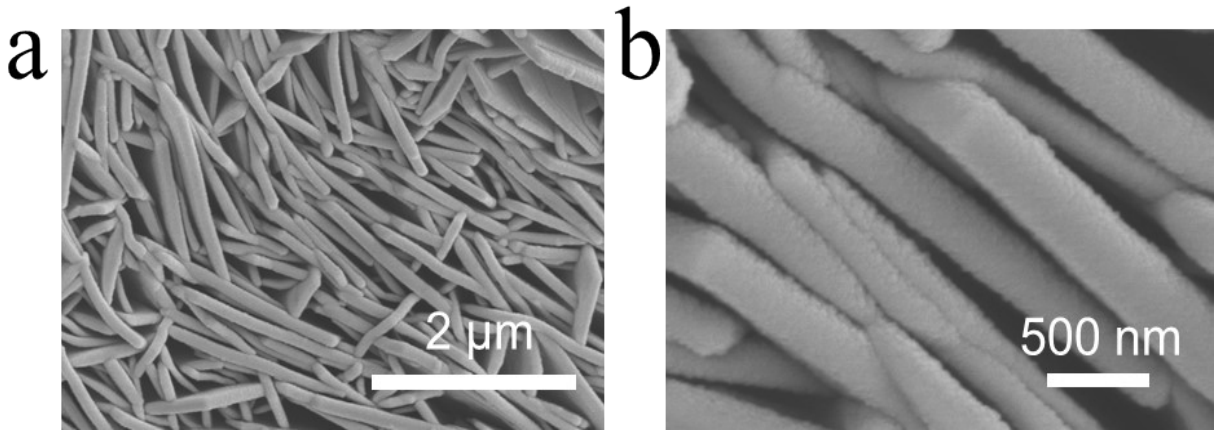

Fig. S14. (a) Low- and (b) high-magnification SEM images of V-NiFe LDH/NF after stability test in 1 M KOH + seawater.

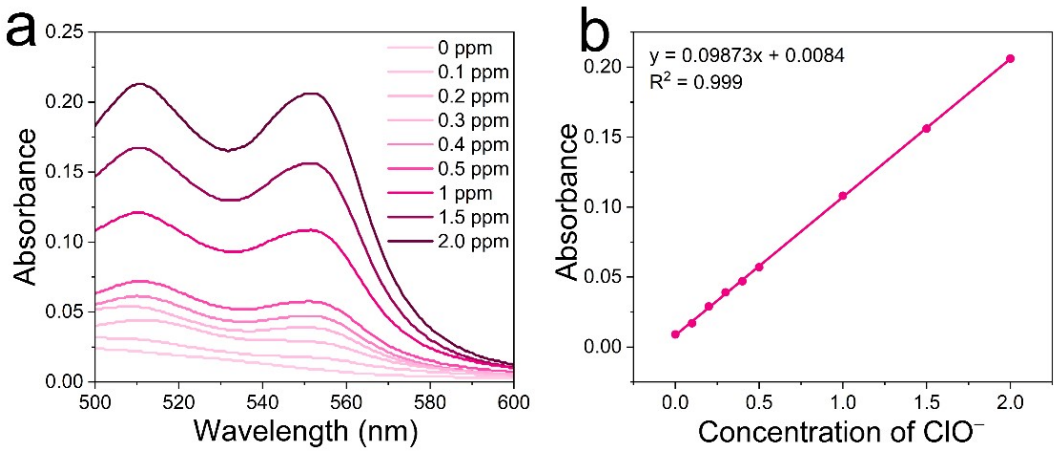

Fig. S15. (a) UV-vis absorption spectra of various active chlorine concentrations and (b) corresponding linear fit.

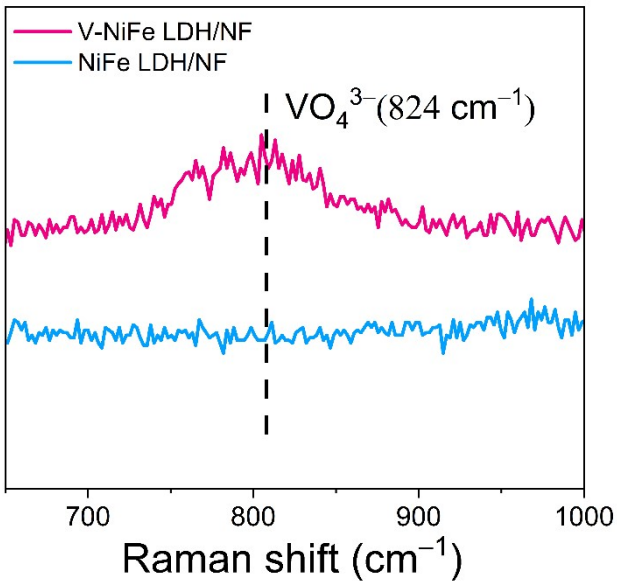

Fig. S16. In-situ Raman spectra collected for NiFe LDH/NF and V-NiFe LDH/NF during the ASO process.

Table S1. Ion compositions of the natural seawater (before the seawater alkalization) and alkaline seawater (after the seawater alkalization) used in this work.

Species	Conc. [mg L^{-1}] for natural seawater	Conc. [mg L^{-1}] for alkaline seawater
Mg^{2+}	746.84	0.65
Ca^{2+}	265.93	9.26

Notes: The seawater was collected from Huangdao district, Qingdao city, China. The pH value for natural seawater was around 7.95, and pH for alkaline seawater was around 14.00.

Table S2. Comparison of the OER performance of V-NiFe LDH/NF with other reported seawater OER electrocatalysts.

Catalyst	Electrolyte	Current Density (mA cm^{-2})	Overpotential (mV)	Ref.
V-NiFe LDH/NF	**1 M KOH + seawater**	**1000**	**368**	**This work**
$NiMoO_4$@NiFe LDH	1 M KOH + seawater	500	349	*Sustain. Energy Fuels*, 2022, **6**, 5521−5530
NiFe LDH@PP	1 M KOH + seawater	1000	390	*J. Mater. Chem. A,* 2025, **13**, 25329–25334
Fe-NiS/NF	1 M KOH + seawater	1000	420	*Inorg. Chem.*, 2023, **62**, 7976−7981
RuNi-Fe_2O_3/IF	1 M KOH + seawater	1000	497	*Chin. J. Catal.*, 2022, **4**, 2202−2211
Ni_2P-Fe_2P/NF	1 M KOH + seawater	1000	431	*Adv. Funct. Mater.*, 2021, **31**, 2006484
Pd@NiFe LDH/NF	1 M KOH + seawater	1000	370	*J. Colloid Interface Sci.*, 2025, **700**, 138388
B-Co_2Fe LDH/NF	1 M KOH + seawater	1000	415	*Nano Energy*, 2021, **83**, 105838
S-(Ni,Fe)OOH/NF	1 M KOH + seawater	1000	462	*Energy Environ. Sci.*, 2020, **13**, 3439−3446
RuMoNi/NF	1 M KOH + seawater	1000	470	*Nat. Commun.*, 2023, **14**, 3607
NiFeO-CeO_2/NF	1 M KOH + seawater	1000	408	*ACS Nano*, 2023, **17**, 16008−16019
TS-NiFe LDH/NF	1 M KOH + seawater	1000	412	*Small*, 2024, **20**, 2311431
F-$FeCoP_v$@IF	1 M KOH + seawater	1000	370	*Appl. Catal. B: Environ.*, 2023, **328**, 122487
CDs-Mn-Co_xP/NF	1 M KOH + seawater	1000	476	*Small*, 2024, **20**, 2402478
Mn-FeP_v/IF	1 M KOH + seawater	1000	395	*Small*, 2024, **20**, 2308613

Table S3. Comparison of the stability at different current density for V-NiFe LDH/NF with previously reported electrocatalysts in alkaline seawater.

Catalyst	Electrolyte	Current Density (mA cm^{-2})	Time (h)	Ref.
V-NiFe LDH/NF	**1 M KOH + seawater**	**1000**	**1000**	**This work**
$NiMoO_4$@NiFe LDH	1 M KOH + seawater	100	80	*Sustain. Energy Fuels*, 2022, **6**, 5521−5530
NiFe LDH@PP	1 M KOH + seawater	1000	800	*J. Mater. Chem. A,* 2025, **13**, 25329–25334
Fe-NiS/NF	1 M KOH + seawater	500	25	*Inorg. Chem.*, 2023, **62**, 7976−7981
NiFe LDH@NiFe-Bi/NF	1 M KOH + seawater	1000	600	*Mater. Today Phys.*, 2025, **50**, 101612
RuNi-Fe_2O_3/IF	1 M KOH + seawater	100	100	*Chin. J. Catal.*, 2022, **4**, 2202−2211
NF/NiFe LDH@ TPP	1 M KOH + seawater	1000	500	*ACS Appl. Nano Mater.*, 2025, **8**, 1332−1337
B-Co_2Fe LDH/NF	1 M KOH + seawater	500	100	*Nano Energy*, 2021, **83**, 105838
S-Ni/Fe(OOH)/NF	1 M KOH + seawater	300	100	*Energy Environ. Sci.*, 2020, **13**, 3439−3446
RuMoNi/NF	1 M KOH + seawater	500	300	*Nat. Commun.*, 2023, **14**, 3607
NiFeO-CeO_2/NF	1 M KOH + seawater	1000	200	*ACS Nano*, 2023, **17**, 16008−16019
TS-NiFe LDH/NF	1 M KOH + seawater	1000	350	*Small*, 2024, **20**, 2311431
CDs-Mn-Co_xP/NF	1 M KOH + seawater	500	100	*Appl. Catal. B: Environ.*, 2023, **328**, 122487
Mn-FeP_v/IF	1 M KOH + seawater	500	200	*Small*, 2024, **20**, 2402478
NiFe-$C_2O_4^{2-}$ LDH/NF	1 M KOH + seawater	1000	500	*J. Colloid Interface Sci.*, 2024, **662**, 596−603
NiFe LDH-CeW@NFF	1 M KOH + seawater	1000	100	*Appl. Catal. B: Environ.*, 2023, **330**, 122612
Cr-Co_xP/NF	1 M KOH + seawater	100	140	*Adv. Funct. Mater.*, 2023, **33**, 2214081
R-CoC_2O_4@MXene	1 M KOH + seawater	10	100	*Adv. Funct. Mater.*, 2022, **32**, 2201081

Mn-doped Ni_2P/Fe_2P/NF	1 M KOH + seawater	500	200	*J. Chem. Eng.*, 2023, **454**, 140061
Pt-Co-Mo/NF	1 M KOH + seawater	500	12	*Appl. Catal. B: Environ.*, 2022, **317**, 121762

Table S4. Element analysis of V-NiFe LDH/NF and NiFe LDH/NF after stability test by ICP-OES.

Catalyst	Element	Element concentration (mg/L)
V-NiFe LDH/NF	Ni	0.011
	Fe	0.032
	V	0.002
NiFe LDH/NF	Ni	0.07
	Fe	0.14

Table S5. Comparison of the cell tolerance at different current density for V-NiFe LDH/NF with previously reported electrocatalysts in alkaline seawater.

Catalyst	Electrolyte	Current Density (mA cm^{-2})	Time (h)	Ref.
Pt/C/NF||V-NiFe LDH/NF	**1 M KOH + seawater**	**500**	**150**	**This work**
Co-Fe_2P/NF||Co-Fe_2P/NF	1 M KOH + seawater	100	24	*Appl. Catal. B: Environ.*, 2021, **297**, 120386
Fe-doped Ni_2P||Fe-doped Ni_2P	1 M KOH + seawater	500	100	*Adv. Funct. Mater.*, 2024, **34**, 2404254
CoFeOF/NF||CoFeOF/NF	1 M KOH + seawater	400	140	*Chem. Eng. J.*, 2024, **480**, 146545
Pt/C/NF||Ce-NiFe LDH/NF	1 M KOH + seawater	300	120	*J. Energy Chem.*, 2024, **91**, 306−312
FeMo-NiP_x/NF||FeMo-NiP_x/NF	1 M KOH + seawater	400	200	*Inorg. Chem. Front.*, 2024, **11**, 498−507
Ni_3N@C||Ni_3FeN@C	1 M KOH + seawater	100	100	*J. Mater. Chem. A*, 2021, **9**, 13562−13569.
F-$FeCoP_v$@IF||F-$FeCoP_v$@IF	1 M KOH + seawater	120	100	*Appl. Catal. B Environ.*, 2023, **328**, 122487
NiPS/NF||NiPS/NF	1 M KOH + seawater	200	60	*J. Energy Chem.*, 2022, **75**, 66−73
$(Fe_{0.74}Co_{0.26})_2P/Ni_3N$/NF||$Fe_2P/Ni_3N$/NF	1 M KOH + seawater	100	70	*Small*, 2023, **19**, 2207082